IEEE Journal of Translational Engineering in Health and Medicine

Received 8 September 2016; revised 9 December 2016 and 1 February 2017; accepted 26 February 2017.
Date of publication 26 January 2018; date of current version 10 May 2018.

Digital Object Identifier 10.1109/JTEHM.2017.2688458

Effectively Measuring Respiratory Flow With Portable Pressure Data Using Back Propagation Neural Network

DAYONG FAN[1], JIACHEN YANG[1], JUNBAO ZHANG[2], ZHIHAN LV[3], (Member, IEEE), HAOJUN HUANG[4], JUN QI[5], AND PO YANG[5], (Member, IEEE)

[1]School of Electronic Automation and Information Engineering, Tianjin university, Tianjin 30072, China
[2]School of Computer Science, Zhongyuan University of Technology, Zhengzhou 45007, China
[3]School of Electronic Information, Wuhan University, Wuhan 430072, China
[4]Department of Computer Science, Liverpool John Moores University, Liverpool L3 5UA, U.K.
[5]Shenzhen Institutes of Advanced Technology, Chinese Academy of Sciences, Shenzhen 518055, China

CORRESPONDING AUTHORS: J. ZHANG (cquard@163.com) AND P. YANG (p.yang@ljmu.ac.uk)

This work was supported in part by the National Natural Science Foundation of China under Grant 61303001 and in part by the National Science Foundation of China under Grant U1504614.

ABSTRACT Continuous respiratory monitoring is an important tool for clinical monitoring. The most widely used flow measure device is nasal cannulae connected to a pressure transducer. However, most of these devices are not easy to carry and continue working in uncontrolled environments which is also a problem. For portable breathing equipment, due to the volume limit, the pressure signals acquired by using the airway tube may be too weak and contain some noise, leading to huge errors in respiratory flow measures. In this paper, a cost-effective portable pressure sensor-based respiratory measure device is designed. This device has a new airway tube design, which enables the pressure drop efficiently after the air flowing through the airway tube. Also, a new back propagation (BP) neural network-based algorithm is proposed to stabilize the device calibration and remove pressure signal noise. For improving the reliability and accuracy of proposed respiratory device, a through experimental evaluation and a case study of the proposed BP neural network algorithm have been carried out. The results show that giving proper parameters setting, the proposed BP neural network algorithm is capable of efficiently improving the reliability of newly designed respiratory device.

INDEX TERMS Respiratory monitoring, mainstream, airway flow, respiratory tube, BP neural network.

I. INTRODUCTION

Respiration is an important physiological process which can maintain the vital signs of people stability. Respiratory diseases, such as asthma, chronic rhinosinusitis, bronchiectasis and obstructive sleep apnea, are widely prevalent all around the world. According to the survey from WHO [1] in 2016, over 235 million people suffer from asthma and over 3 million people die each year from chronic obstructive pulmonary disease (COPD). To effectively and accurately assess cardiorespiratory functions, respiratory monitoring is a key component during the administration of respiratory diseases and intensive care unit [2]–[4].

Various techiniques have been used to measure respiratory flow by now, which can be categoried as two ways: direct-mode [5], [6] and indirect mode [12]–[14]. The direct way of measuring respiratory flow is typically achieved by utilising respirometry devices for monitoring airflow, including pneumotachorgraph, heated thermistor, and anemometry or nasal cannulae connected to a pressure sensor [5]. For instance, we have made some progress in the CO_2 concentration detected based on the NDIR technology [7]–[9] and the accuracy of CO_2 concentration monitoring device with pyroelectric sensor can be up to 0.23 mmHg [10], [11]. Due to the advantage of direct connection and close measure to the patient airway, these devices are able to accurately measure people's pulmonary function and further precisely deliver monitoring their respiratory flow. But this method is easy to cause the respiratory pipeline to be polluted, so the precision of the measurement is affected. The indirect way of monitoring respiratory flow can rely on detecting chest or

abdomincal movements using respiratory inductance plethysmography (RIP), strain usages or magnetometers [12]–[14]. In comparison with direct-mode, due to ease of attachment and comfort, indirect approaches are more suitable to continuous respiratory monitoring in clinics. However, it is limited by its relatively low accuracy and slow responses to patients. Considering that accuracy is top priority of most respiratory monitoring systems, in this article we chose direct way of measuring respiratory.

For direct-mode approaches, they require the systems to pay great attention to accuracy, calibration, repeatability, and precision for strict laboratory measurements. The most widely used flow measuring device is nasal cannulae connected to a pressure transducer. The operation principle of pressure sensors for measuring respiratory flow is that the volume flow can be measured by the pressure drop via a flow element, which involves sensing a flow-induced differential pressure. The Philips-Respironic family [15] has made some early attempts on adding pressure-sensing ports on both the proximal and distal sides of the optical window in a mainsteam CO2 cuvette. For daily use, due to the pursuit of the device's accuracy, the portability of the breathing machine is greatly decreased so it is not easy to carry, and needs higher requirements for the environment, so the research on a small volume, simple power suppied mode and the device which can adapt to various environmental respiration monitoring are very necessary.

In this paper, we proposed a pressure sensor based measuring device which combines the designed airway tube with breathing circuits. In order to accurately monitor the physical condition of patients, we designed a device which combines the respiratory tube with the breathing circuit. Our system uses piezoresistive silicon sensor to measure airway flow [16]. Considering some issues may affect the accuracy of our experimental results, we adopted mainstream airway adapter to make the results in real-time and with higher fidelity. Accurate sensor and stable circuits are chosen to enhance the accuracy of our experimental results. The mainstream device can be used for monitoring the respiratory flow in patient care, anesthesia, and transport. By confirming the device can produce stable signals, we carried out targeted experiments depending on the proposed device. On the basis of analyzing the experiment data, we proposed the algorithm which is based on the back propagation (BP) neural network, and BP neural network model is also established. We carried out targeted experiments by using the proposed device and confirmed that the device was reliable. The main contributions of this paper are below:

1) A cost-effective portable pressure sensor based respiratory measureing device is designed. This device has a new airway tube design, which enables that the pressure drop can efficiently emerge after the air flowing through the airway tube.
2) A new back propagation (BP) neural network based algorithm is proposed to stablise the device calibration and remove pressure signal nosie, for improving the reability and accuracy of proposed respiratory device.
3) A through experimental evaluation and a case study of proposed BP neural network algorithm have been carried out. The results show that giving a proper parameters setting, the proposed BP neural network algorithm is capable of efficiently improving the reliability of new designed respiratory device.

The remainder of this paper is organized as follows: Section 2 introduces the related work to respiratory flow measurement. Section 3 presents the detailed design of device and method and analysis of calibiration and testing. Section 4 describes the experimental analysis and comparisons, and Section 5 concludes the paper.

II. RELATED WORK

A. MAINSTEAM DIFFERENTIAL PRESSURE FLOW SENSORS

Given the portability and the requirement of clinical respiratory monitoring, the most widely used flow measurement devices are the Fleisch or Lilly-type differential pressure pneumotach [17], [18] with a heated microtube or screen orifice. For enabling faster signal response and precise time alignment between the flow and gas concentration signal, these pressure sensor based respiratory devices are mainstream, located directly on the patient's endotracheal tube.

The measurement of airway flow is based on the method of measuring differential pressures between two pressure ports which are placed on the airway tube. The Bernoulli law is used to determine flow based on the differential pressure:

$$\frac{1}{2}\rho v_A^2 + \rho_A = \frac{1}{2}\rho v_B^2 + \rho_B \tag{1}$$

Where ρ is the density of air, v_A and v_B are the velocities of the airflow at the two different ports, ρ_A and ρ_B are the magnitude of the pressure [18].

Usually, it is quite simple and precise for the monitoring of airway flow by measuring the differential pressure. However, a common problem in many cases is that the pressure signals acquired by using the airway tube may be too weak and contain some noise, further leading to huge errors in respiratory flow measures. The acquisition of pressure signals has a strong relationship with the airway tube [29]. As such, the airway tube is the basis of the system to acquire pressure signals, the structure of airway tube must be taken into consideration and a reasonable pipeline directly affects the accuracy of measurement results.

B. ARTIFICIAL NEURAL NETWORKS

Due to huge uncertainty and noise of sensor signals in respiratory flow measures, it is indispensable to employ some advance algorithms to improve the classification of respiratory states. For respiratory states estimation, many ANN based classification methods have been proposed to deal with various type of sensing signals, for instance, ANN with multilayer perceptron [19], Fuzzy logic with Fuzzy Knowledge

IEEE Journal of Translational Engineering in Health and Medicine

Base Controller (FKBC) [19], Black propagation neural networks (BPNN) [20], K-Nearest Neighbour (KNN) supervised learning classifer and Support Vector Machine (SVM) [21]. Owning to the capability to solve nonlinearly separable problems and the flexibility to implement on-chip processor, Artifical Neural Networks (ANN) [19], [20] are frequently used for classification. The conventional ANN can achieve the indispensable conversion and clustering operations routinely and concurrently.

In this work, BP neural network (BPNN) algorithm [22], [23] are investigated as a potential way for enhancing the efficiency and accuracy of respiratory flow meausres. BP neural network has many advantages, such as that it has the characteristics of self-learning and it is adaptive. Moreover, BP neural network has robustness and generalization which makes it widely used in many fields [24], [25], such as function approximation, pattern recognition, image processing, forecasting and other fields. The basic principle of the neural network is to put input vector (provided by the training sample data) through a series of hidden layers [26] and then it will build the relationship between input and output data. The forward transmission of input data and the reverse transmission of output error data form the information cycle of BP neural network. BP algorithm modifies the connection weights of neurons on the basis of output error data. The purpose is to make output error data to reach an expected range. Hebb learning rule [27] and Delta learning rule are the two very classic learning rules for neural network learning.

III. METHOD

A. DESIGN OF THE MAINSTREAM DEVICE

Given the portability and the requirement of clinical respiratory monitoring, the mainstream device has been designed with three functional modules (see Fig.1).

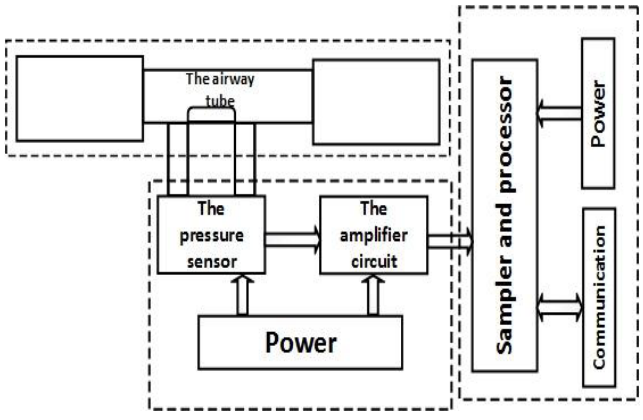

FIGURE 1. Structure of mainstream device.

The pressure sensor is a piezoresistive silicon sensor in which the piezoresistors are arranged in the Wheatstone bridge configuration to achieve higher voltage sensitivity and low temperature sensitivity [28]. Since the signals which are acquired from the sensor may be too weak and noisy, a band-pass filter amplifying circuit is designed to intensify pressure signals and filter the noise [17].

In general, in this device, sampling and amplifying circuits are integrated in the same module, and the system can directly filter on the lower position machine. The design helps to improve the portability of the device and high integrate of the system to reduce the external circuit interference which can generate electromagnetic wave of the signal. At the same time, the two modules are independent power supplied to improve the anti-interference performance. So the device is more concise, stronger anti-interference compared to the similar equipment.

The design of this device has also considered other environmental issues' impacts. First, regarding the influence of temperature on respiratory equipment accuracy, the device we designed will be used in normal daily environmental temperature conditions. So a cost-effective silicon piezoresistive pressure sensor MS4515 with temperature compensation circuit is chosen to be integrated in this device. The operating temperature range of this sensor is between 0 to 60 degrees. In comparing with common pressure sensors, our device has the feedback circuit with temperature compensation, and the pressure curve is calibrated after compensating. Also, the analog signal in our device is converted by alternating current AD and direct current DA. The second issue is the effect of humidity on the precision of the sensor. Some initial experiments are carried out to evaluate the change of humidity impacting on the carrier signal of AC component and DC component. The experimental results show that humidity change mainly affects the strength of AC component; and the airflow intensity change mainly causes the oscillation of the DC component. Therefore, we have used 3D printing technology to make the pipeline replaceable, so it is simply and conveniently for users to replace the pipeline, which is seriously polluted. Finally, in order to reduce the effects of the foreign body produced when breathing we added filter screen at the front of the pressure ports. In order to reduce the influence of the breathing precision, we calibrated every pipeline after installing filter screen, and saved the calibrated parameters.

B. DESIGN OF BP NEURAL NETWORK MODEL

When we collected the output data of the sensor, we found that the data were a set of discrete voltage values; and as our device is portable, its performance will be reduced compared with the professional equipment, so if we want to make use of these data for further processing, we must select appropriate algorithm to make up for declining accuracy caused by simple hardware equipment, and make the results closer to the actual testing result.

Usually, interpolation method can fit the data of the sensor [29] or the least square method [30], [31]. During the experiment, the application of interpolation fitting requires the fitting curve through all the points, but our portable equipment is not high precision as professional equipment,

so the fitting accuracy and resolution of the original data are not up to the requirements of professional equipment. If the interpolation method is used to fit the curve, the curve will appear a very obvious inflection point, which makes the flow in some specific appear relatively large error. Using the least square method will also appear such a situation. Because the least square method is restricted by the function, so sometimes it will not exactly fit the desired function. It requires applying a more professional fitting algorithm to achieve the results of fitting and make the equipment to achieve the best response to the change of the weak airflow. Also for the universal ventilator sensors, the typical range of the fitting is between 0 and 1 psi, the sampling points in this range can satisfy the condition of least squares fitting. But in some places where the air changes are relatively large so the application of piecewise least square method will have a steep line, which leads to inaccurate measurement results. Even worse, in the actual measurement process, we found that the maximum pressure generated by breathing is far less than the 1psi. In this experiment, we selected 2inH2O as the maximum range of the sensor. It is proved that this measurement range can well meet the needs of the measurement, the decrease of the measurement range of the sensor can shorten the sampling accuracy of the least square method to increase the further error.

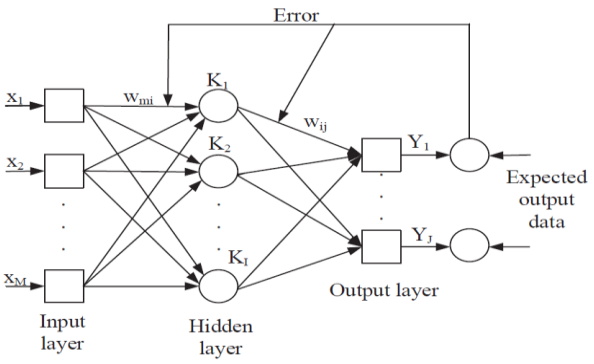

FIGURE 2. Three layers BP neural network.

The specific function of the network topology does not restrict BP neural network, it is simple, and has high accuracy, and it has strong maneuverability, so we selected BP neural network as fitting function to fit the data. In this paper BP neural network model is designed as a three layers network (see Fig.2), which includes input layer, output layer and hidden layer. When the actual output data are not in conformity with the expected output data, the algorithm turns to transmit in the opposite direction, from the output layer to the hidden Layer then to the input layer and corrects weights and thresholds of each layer according to the predictive error gradient. In this work, the selected excitation function is hyperbolic tangent sigmoid transfer function; the training function is trainlm training function.

C. ANALYSIS OF THE AIRWAY TUBE

Considering that the mainstream device must be portable and real-time, so it is designed by combining airway tube with breathing circuits. The airway flow is monitored by sampling pressure, which has a strong relationship with the airway tube. The main consideration of the airway tube design is that the pressure drop can emerge after the air flowing through the airway tube. The design of airway tube is based on the Bernoulli law and the continuity law:

$$\rho s_A \upsilon_A = \rho s_B \upsilon_B = m \tag{2}$$

where s_A and s_B are the cross sectional area, ρ is the density of air, v_A and v_B represent the velocity of the two ports, m is the mass of the airflow.

According to the equation 1 and equation 2, we can calculate the pressure drop Δp:

$$\Delta p = \rho * \frac{s_A^2 - s_B^2}{2 s_A^2 s_B^2} * Q^2 \tag{3}$$

where Q is the volume flow.

Therefore, we should know the pressure drop and then we can calculate the respiratory flow.

In our previous study [9]–[11], a mesh generator (Gambit) was used to design a computational fluid dynamics mesh of the airway adapter and a computational fluid dynamics solver (Fluent) was used to simulate the computational model. But in application, we utilize this mesh generator method to give an initial experimental evaluation of potential pressure ports position, with an approximate range. And then, we adapt control variable methods to practically evaluate the best position during experiments. This is a calibration procedure to determine the final position of the pressure hole and make the difference of the pressure reach the maximum.

In order to obtain the pressure signal, the key point lies in the design of airway tube. And pressure ports and throttling device are hardly to generate the pressure drop with high accuracy. Pressure signals are acquired from pressure ports and the pressure drop forms before and after throttling device. Then we need to select the appropriate location of the pressure ports and the throttling device. In response to this, several different design solutions of airway tube are designed as shown in Fig.3.

In Fig.3, the numbers represent the locations of pressure ports before and after throttling device, and letters represent the different locations of the throttling device. Then we tested the relationship by using these designed airway tubes. Finally, we chose the appropriate airway tube for the mainstream device.

D. ANALYSIS OF CALIBRATION

The typical calibration techniques are important to remove the noisy raised from the positions of differential pressure sensors. In this research work, we have taken some actions in designing the pipeline and the position of pressure sensors

IEEE Journal of Translational Engineering in Health and Medicine

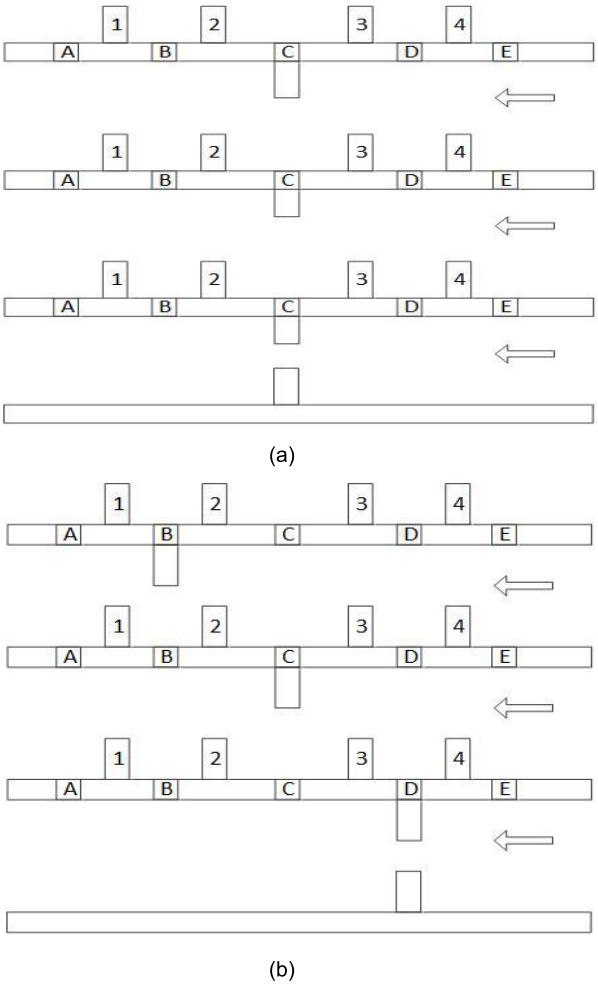

FIGURE 3. Different settings of pressure ports and throttling device. (a) Design (1) of location of the pressure ports. (b) Design (2) of location of the pressure ports.

instead of utilizing traditional algorithm calibration procedures. The focus of this work is to investigate the feasibility of using neural network algorithm in improving the measures of a cost-effective wearable device. We assume the output data of BP neural network are a vector which is J in length. The actual output of the network is:

$$Y(n) = \left[\upsilon_j^1, \upsilon_j^2, \ldots, \upsilon_j^J\right] \tag{4}$$

where υ represents the output data.

The expected output of the network is:

$$d(n) = [d_1, d_2, \ldots, d_J] \tag{5}$$

where n is iterations.

The iterative error signal is defined as:

$$e_j(n) = d_j(n) - y_j(n) \tag{6}$$

The error energy is defined as:

$$e(n) = \frac{1}{2}\sum_{j=1}^{J} e_j^2(n) \tag{7}$$

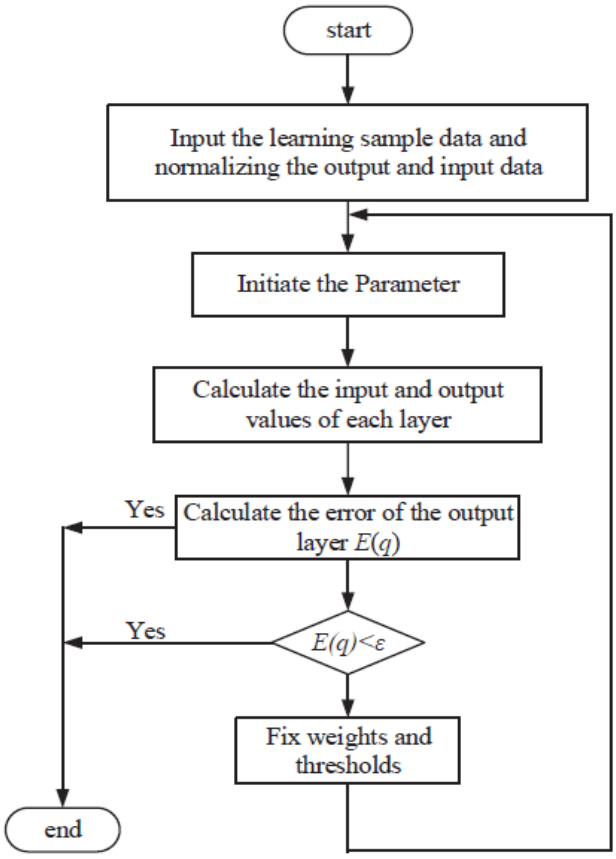

FIGURE 4. Process of BP neural network.

Then we can represent the implementation steps in the form of the flow chart (see Fig.4).

For fitting the function curve of voltage and flow rate accurately, it is very important to select the appropriate excitation function and training function. In this paper, we chose sigmoid function as the excitation function, and use Levenberg-Marquardt (LM) algorithm to train.

1) EXCITATION FUNCTION

The excitation is defined as:

$$tansig(n) = \frac{2}{e^{-2n}} - 1 (-1 < tansig(n) < 1) \tag{8}$$

The output of the function ranges from -1 to 1 as shown in Fig.5.

2) TRAINING FUNCTION

We chose Levenberg-Marquardt (LM) algorithm to train data. LM algorithm is a kind of fast algorithm which uses the standard numerical optimization, and it is the combination of the gradient descent and Gauss-Newton method. LM algorithm not only has the local convergence of Gauss-Newton method, but also has the global character of the gradient descent method.

LM algorithm uses the information of two-order derivative, so it is much faster than the gradient descent method.

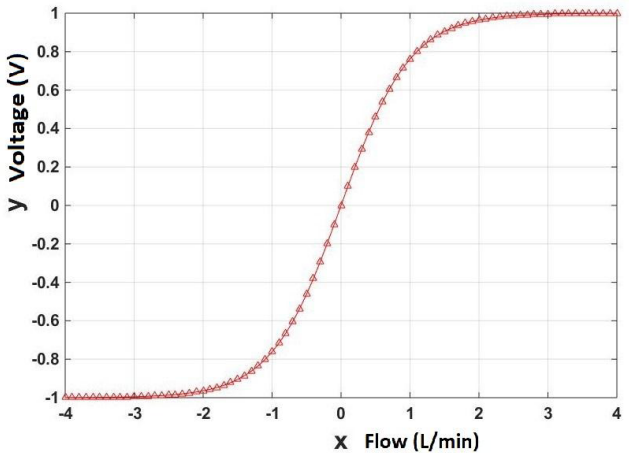

FIGURE 5. Function of Tan-sigmoid.

The vetor of weights and thresholds is:

$$x = [\omega_{ih}(1,1)\ldots\omega_{ih}(h,i), b_h(1)\ldots b_h(h)\,\omega_{ho}(1,1)\ldots b_o(0)]^T \quad (9)$$

So the vector which is composed by updated weights and thresholds is:

$$x(k+1) = x(k) + \Delta x \quad (10)$$

Where Δx indicates the change of weights and threshold. LM algorithm is the improved algorithm of the Newton-Gauss method which is defined as:

$$\Delta x = -\left[J^T(x)\,J(x) + \mu I\right]^{-1} J^T(x)e \quad (11)$$

Where $J(x)$ is Jacobian matrix, u is damping coefficient, I is unit matrix.

LM algorithm is similar to gradient descent method, after each iterating, reduces the value of coverages. So when the algorithm is close to the target error, it is gradually close to Gauss-Newton method.

LM algorithm is an efficient algorithm whose basic idea of the iterative process allows the error search along the direction of deterioration. At the same time, in order to achieve the purpose of optimizing the network weights and thresholds, we adopted gradient descent method and adaptive adjustment method, which can make the network convergence and improve the generalization ability and convergence speed of the network.

IV. RESULTS AND DISCUSSION

A. DESIGN OF THE AIRWAY TUBE

Using the airway tubes made by different design solutions, we began to do experiments. After 1 min of warming up while the system was powered on, we passed into air at one velocity. We collected the data from the system for 1min after the airflow stabilizing. And then we passed different velocities of air and did the same experiments by using the same airway tube. We have added the analysis of different velocity values in the section 4.4 Table 2 and Table 3. In section 4.1, it only shows an initial experimental estimation for observing the performance of the different pressures of the pipeline.

Secondly, we verified the relationship between signals and the location of pressure ports and the throttling device. On the basis of simulation experiments, we have made different types of pipelines. We selected different airway tubes to do the experiment and finally we chose the reasonable scheme which had the most significant effect of differential pressure to design the airway tube. After repeated experiments and combined with simulation results, we finally determined the outer diameter of the pipeline is 16mm, the internal diameter is 12mm, the length of the pipeline is 80mm, the pressure hole diameter is 4mm, the two-pressure hole center distance is 18mm.

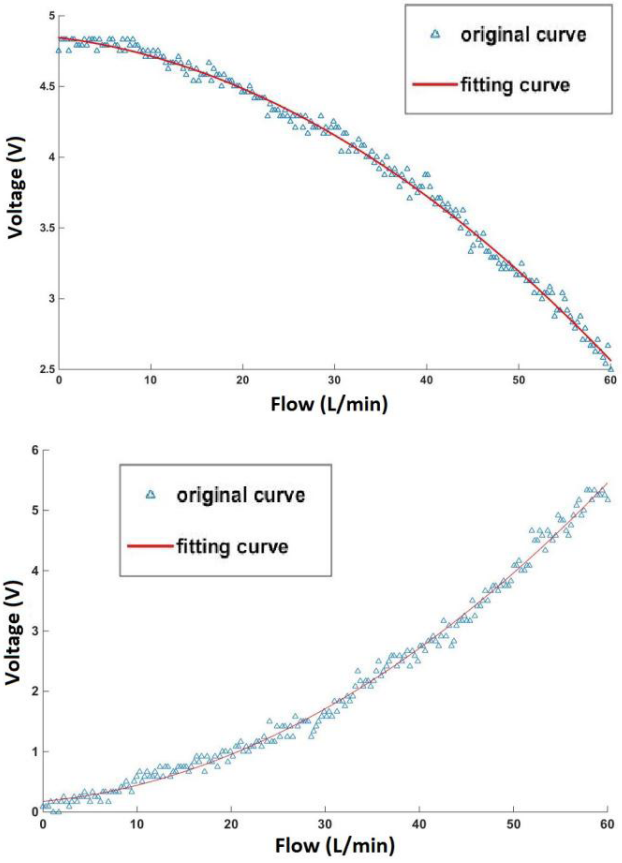

FIGURE 6. Relationship between flow and voltage.

While measuring the exhaled gas flow, the control variable method was used to eliminate the interference. We just changed the velocities of airflow without any other changes. For our simulation, we simulated natural breathing. By changing the flow varying from 0L/min to 60L/min, we gathered data from both channels of the pressure transducer. Fig.6 shows the changing trends when sampling from each pressure port. As the Bernoulli law describes, when air flows through the throttling device, the airflow slows down and the pressure sampling from the proximal port increases (see Fig.6 (a)).

IEEE Journal of Translational Engineering in Health and Medicine

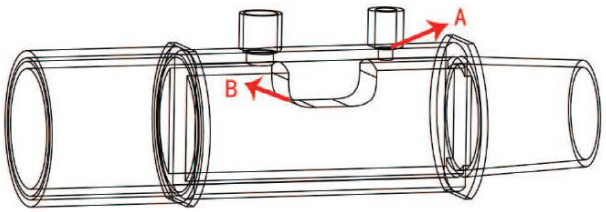

FIGURE 7. Structure of airway tube.

After the airflow passes through the throttling device, the pressure on the distal decreases (see Fig.6 (b)). With repeated experiments using the airway tube, the desired results were achieved which suggested that the new airway tube that we selected can be used to accurately monitor airway flow. According to these designs, the structure of airway tube is designed by mechanical drawing software (see Fig.7).

In Fig.7, A represents the improvement of pressure ports and filter screen is set to avoid the interference caused by condensed water and patient secretions. B represents the chamfer edge of the throttling device, turbulence will be caused when the airflow gets to the right-angle tube wall. In consideration of this case, so we changed the edge of the throttling device. We set the chamfer edge of the throttling device, which can make the airflow a smooth transition so as to avoid turbulence. And next we manufactured the tube adopting photosensitive resin material that can form a smooth surface through 3D print technology.

After the design of the airway tube, we can acquire pressure signals sampling from the airway tube by combining with breathing circuits. However, if the pressure signals are too weak, it will have an impact on our results. In addition to the design of airway tube, the amplifier circuit can also be used for intensifying the pressure signals. By comparison, we chose the chip AD8619 and designed the amplifier circuit. In order to acquire better signals, the signals produced by the transducer are filtered through adding the bypass capacitor. The calibration of pressure transducer is one major problem in our study. According to the Bernoulli law, the airway flow is in a tightly correlated exponential relation with the pressure drop. However, though the experimental results followed this pattern, the mainstream device still contains considerable error that the pressure signals may drift. And the signal drift will decrease the accuracy of the mainstream device. Therefore, we only acquired the differential pressure directly between the two pressure ports, after which the differential pressure singles were converted to voltage values (see Fig.8).

B. CALIBRATION AND TESTING

Normally, each ventilator needs a calibration before use. In previous studies, we have designed and experimented different types of ventilators for children, adults, and the elderly. The results show that while the ventilator models can be different, their calibration curves are slightly different. It implies that the choices of different calibration methods

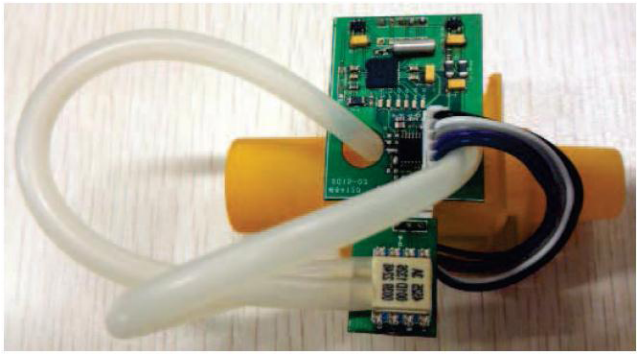

FIGURE 8. Airway tube and breathing circuits.

have no apparent impact on the errors of fitting curves. In this work, we are currently designing a software for automatic calibration of the curve. The standard flow meter is used for calibration.

The experiment focused on the data of 60 groups, with flow changing from 1L/min to 60L/min slowly at the interval of 1L/min to collect the corresponding voltage values. The flow data were divided into two groups, the odd numbers of the flow data were trained and the dual numbers of the flow data were tested.

After training, we inputted testing data to the neural network to describe the shape of the fitting curve and calculate the accuracy index. The neural network used in this calibration consists of two layers, the hidden layer and the output layer. As the design, the hidden layer contains 20 neurons. The iterations are 6 times, and the time is 1s. When the iterations reach 6 times, the value of the gradient is 0.00496. Fig.9 expresses the fitting degree between both of the training and testing data and the real output data. With the increasing of iterations, the minimum mean square error is declining, which is less than when iterations reach 6 times. Then it will stop learning, the specific curves will finally get.

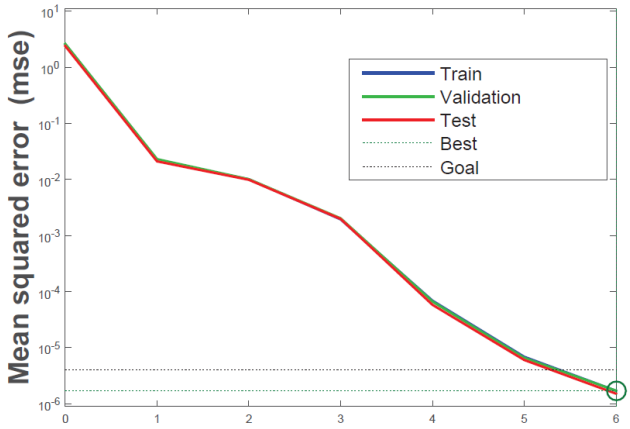

FIGURE 9. Predictive and actual data.

Fig.10 shows the condition of the network during the learning process. We can see the specific gradient change of LM

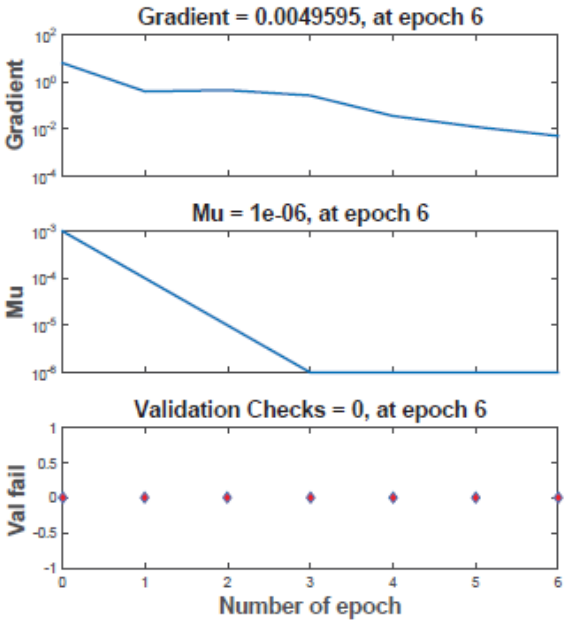

FIGURE 10. Condition of the network.

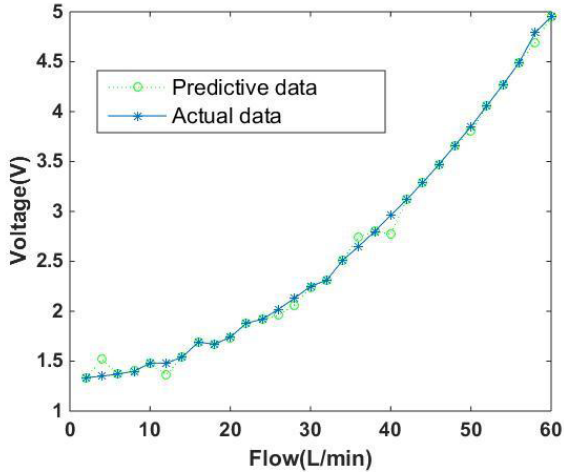

FIGURE 11. Predictive and actual data.

algorithm with the increase of iterations directly. Mu is the mean of normal distribution, which is similar to error.With the increase of iterations, if the error value increases, then the mu value will increase accordingly, so when the value of mu is too large, the learning process should be stopped.

Fig.11 shows the output data which are acquired after BP neural network training and from the experiment respectively. We can observe the error directly. The distance between the majority of the output data and the actual output data is short, only a small numbers of data happen to jump. The trend of fitting curve will not be affected and the relationship between the flow rate and the voltage will be reflected by the trend of the curve. So we can conclude that the training of the neural network is accurate.

However, a noticeable issue is that the data in Fig.11 we collected can be fitted by traditional calibration methods like least square method in the literature [30], [31]. It is because these data in Fig.11 are mainly collected from a controllable lab environment, not from practically uncontrollable environments. The advantages of proposed BP neural network over traditional least square methods on accuracy have been not fully reflected with these data set. However, the device of our developed in this paper is a low-cost wearable equipment for uncontrollable environments. It means that the data from practical application may be more sensitive and noisy. The utilisation of BP neural network has some advantages over traditional calibration methods in these cases. In the future work, we will take more experiments on real applications and validate the proposed BP methods.

Regarding the measure of overall accuracy of the data of 60 groups, we use RMSE (Root Mean Square Error) and RE (Range of Error), Absolute Error (AE) to measure the predicted voltage data over 60 gourps with both our proposed BP neural network method and traditional least square method [30]. The results are shown in Table.1. It could reflect that the over all accuracy performance of our method can reach the same level to the state-of-the-art least square fitting method. Also, we have calculated the absolute error and percentage of error and plotted them in the Fig.12 and 13.

TABLE 1. RMSE and RE arrange of predicted voltage.

Accuracy	Proposed Algorithm	Least Square method [51]
RMSE (V)	0.061	0.059
RE (V)	(-0.17, 0.12)	(-0.19, 0.13)
AE (V)	0.759	0.736

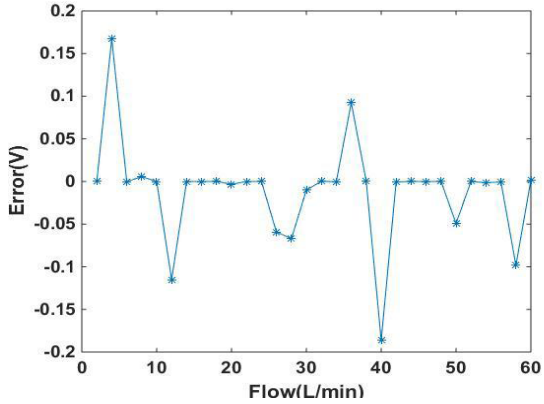

FIGURE 12. AB error of BP neural network.

From Fig.12 we can see that in BP neural network, although the training output data have a relatively large error in individual data, but the fluctuation of training error is very small. Finally we got the absolute error 0.7594, this figure is very intuitive to show the overall accuracy of neural network training. Fig.13 shows the percentage of the error between the testing output and the actual output data after BP neural network processing for 30 sets of testing data.

IEEE Journal of Translational Engineering in Health and Medicine

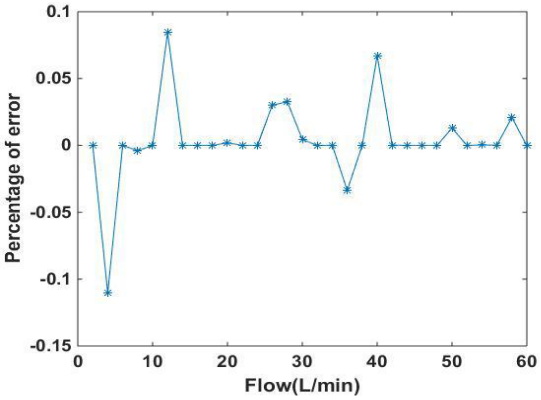

FIGURE 13. Error percentage of BP neural network.

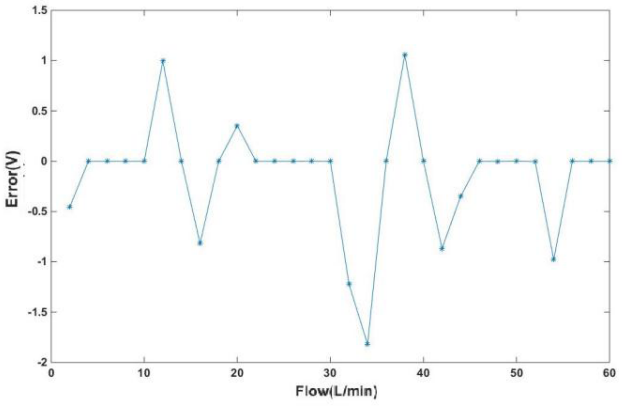

FIGURE 14. AE error of BP neural network with 3 iterations.

The mathematical formula is defined as:

$$\frac{m-n}{m} \tag{12}$$

where m is the testing output data and n is the actual output data. From Fig.13 we can directly infer that the result is corresponded with Fig.12. They both produce large error in 4L/min, 12L/min and 40L/min. But it only happens in the very few data, and it can't affect the good fitting function of our neural network.

C. THE PARAMETER OF BP NEURAL NETWORK

For LM algorithm, the parameters that need to be considered are the hidden layers, threshold, learning step and maximum iterations.

1) THE NUMBER OF THE HIDDEN LAYERS

We select the hidden layer as 5 layers, 50 layers to record the output results in order to analyze and to compare. When the number of layers is selected as 5, the iterations of the neural network are more than 20 times, and sometimes are about 30 times, so we can judge that the fitting effect is not ideal. When the number of layers is 50, the iterations are 3 times, it is satisfactory, but the absolute average value error of BP neural network is 8.9315(see Fig.14), and the value cannot reach a steady state. When the number of hidden layer is 20, the iterations can reach the ideal requirement, and the output error is 0.7594, which means that the neural network expresses a good performance. Indeed, there are some significant errors in Fig.12, however, it is because the flow is unstable and easily affected by many minor factors in practical environment. It is inevitable to remove these errors from device completely in real cases.

2) THE SELECTION OF THE THRESHOLD

The neural network can change the threshold so as to make the fitting better. But taking the smaller the threshold into account, the larger the iterations required. Therefore, the choice of the threshold is based on the actual situation to judge. When the threshold is 4*10–6, the iterations are 6 times and the Sum of absolute value of the testing output data error is 0.7594. And when the threshold is 4*10–7, the iterations are 18 times and the Sum of absolute value of the testing output data error is 0.4266. When the threshold is 4*10–8, the number is 34 and 0.2395 respectively. Finally, combining with the iterations, the selected threshold is 4*10–6.

3) THE SELECTION OF THE LEARNING STEP

In this experiment, we chose different steps, and then chose the best learning step according to the results. We found that the Sum of the absolute value of testing output error data was 0.7594 when the learning step size was 0.01. Comparing with 2.2351 when the learning step was 0.2 and 1.4325 when the learning step was 0.1, we could easily judge that the most suitable step size was 0.01 and then concluded that the Sum of the absolute value of output error became larger and larger with the step size increasing, which indicates that the fitting process was getting worse and worse. In practice, the smaller the learning step size is, the more iterations required to build a neural network, and the longer time it will take, so the result is relatively better. If the learning step is longer, the result of the neural network will be worse, and the number of iterations will be less. To sum up, we select the learning step as 0.01.

D. ANALYSIS OF EXPERIMENT RESULTS

In this experiment, we sat the temperature as 23 $\pm$ 5°C, the relative humidity t <= 2% and kept the Environmental stability, we randomly selected a volunteer for the respiration experiment. The volunteer wore breathing masks (BMC-FM) which connected to our device through hose, the sensor collected respiratory pressure then converted the differential pressure into analog voltage signal. The slave computer sended the analog signal to the host computer through the serial port. Firstly, we filtered the received data to make them stable, to improve the sensitivity of the device, we sat the 12-sampling data as a circular queue, every time we received a new data we putted it into the tail of the queue, and then threw away the first data of the queue, each output data was always the current arithmetic average of the 12 data

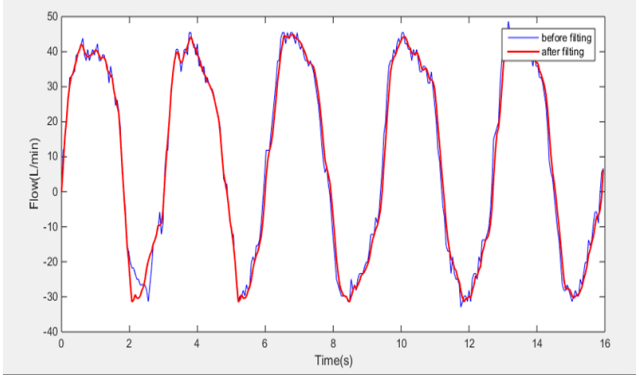

FIGURE 15. Respiratory data curve.

in the queue. After data filtering we got the trend of the breathing which was calculating by the BP neural network Fitting function.

In order to determine the effect of the filtering, we putted the data which were directly received by the serial port into the BP neural network Fitting function to get the trend of the breathing, and then we saw the outcome from Fig.15. From Fig.15 we could see that the jumping of data significantly decreased after flitering.

TABLE 2. Exmperimatal data analysis with our proposed BP neural network method.

Voltage Signals(L/Min)	Mean	Standard Deviation	RMSE
10	10.51	0.054	0.059
15	15.36	0.023	0.026
20	20.52	0.068	0.066
25	25.34	0.052	0.051
30	30.33	0.034	0.036
35	35.17	0.008	0.009

Then we evaluated the accuracy and uncertainty of the system by doing experiments.we chose 6 different flows in this environment and for each flow we did experiment for 10 times. We calculated the mean value and standard deviation by the formula (see TABLE 2):

$$S = \frac{1}{\upsilon}\sqrt{\frac{\sum_{i=1}^{10}(V_i - \upsilon)}{10-1}} \tag{13}$$

where S is standard deviation, V and v is sample data and mean value.

Then we changed BP network filtering function to the least square method to fit the function of the received signal, repeat the above experiment to obtain data (see TABLE.3).

From Table 2 and 3, it appears that with using our proposed BP neural network method and the traditional least square method [30], the standard deviation and RMSE will gradually decrease as the increment of voltage signals. But our proposed methods have lower standard deviation and RMSE than least square method [30]. When the voltage signals are within

TABLE 3. Exmperimatal data analysis with traditional least square method [30].

Voltage Signals(L/Min)	Mean	Standard Deviation	RMSE
10	11.68	0.076	0.081
15	15.36	0.023	0.025
20	22.50	0.084	0.086
25	26.42	0.074	0.073
30	31.71	0.254	0.262
35	36.52	0.039	0.041

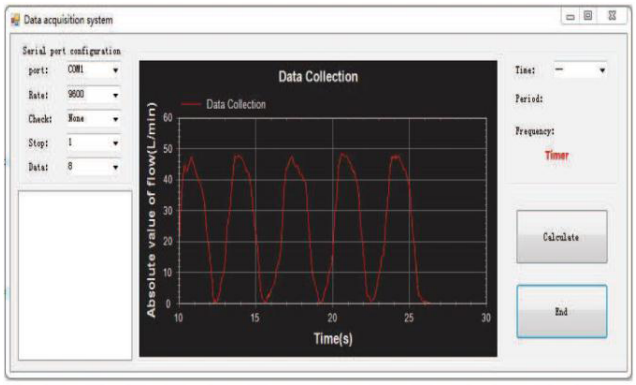

FIGURE 16. The result of the master computer.

low input, this difference is not apparent; but when the voltage signals are outputted within high value, our method performs better accuracy than least square method. It means that the proposed neural network fitting function is capable of making the equipment more stable. Through the above analysis, we got the conclusion that the appropriate filter ing and fitting algorithm could effectively improve the performance of the device. Finally, we examined the continuity and accuracy of the real-time application of the device. We randomly selected an adult in the same respiration experiment and showed his breathing data which was dynamically displayed on the host computer (See Fig.16).

Through the display of the respiratory waveform of the host computer and combined with the previous experiments, we could clearly infer that the waveform is continumm and accurate, the respiratory parameters of the tested person can be measured effectively. Comparing with the parameters of the breathing machine at home and abroad and through the verification of the clinical experiment, we could prove that our device can meet the requirements of accuracy and uncertainty.

V. DISCUSSION AND FUTURE WORK

The experiments show that although the processing speed of the neural network algorithm is slower than the simple method of fitting, but taking into account of the practicality and accuracy of the device, we improved the design of the pipeline and the filter algorithm of the host computer and slave computer to make sure the data are suitable for the

algorithm. At the same time as the respiratory frequency of human is slow, so the speed of the sensor data update is relatively slow too, so the processing speed of the computer is not particularly high, this makes us pay more attention in the design of the algorithm on the processing accuracy rather than processing speed. The most important reason is that because of the instability of the respiratory data so it is difficult to use specific formula to express, which requires us to look for a simple network topology, but also has high accuracy, and it is easy to implement and has strong operability. In the process of training, we only considered the hidden layer, learning step size, the maximum number of iterations and threshold, in the future experiments, we should consider more parameters, and enhanced the reliability of the equipment in the further experiments. Finally considering the temperature and humidity effects on the experimental results, in the future research, we should not only improve the hardware, but also consider improving the software to reduce the cost of the equipment.

In addition, the design of circuit schematic and PCB layout is indeed an important component of this wearable devices. However, the key contribution of this article will mainly the effect of the BP neural network algorithm on the accuracy of the respirator and the perfection of the pipeline; the algorithm is also suitable for other similar principles. So, we did not address the detailed information about hardware design in this article, and rely on our previous work of designing hardware device in [10] and [11]. The involvement of human subjects including respiratory related diseases in further experiment is also very important to verify the efficiency of proposed method. However, in practice, due to the ethical and safety issues, it is very difficult to invite more patients to verify the proposed method in uncontrolled environment. At present, our volunteers are healthy adults who are randomly selected in our university. Hence, the main effect of this paper is to demonstrate the feasibility of applying a BP neural network algorithm and pipeline for improving the performance of a cost-effective wearable device.

Regarding the specification of equipments, we also examine the equipment in other laboratories where they used Bell type gas flow calibration equipment in China Metrology Institute. For our ventilator, we used small standard flow meter and gas tank which can generate a steady flow. It is very convenient for us to carry out experiments to improve the accuracy. Our pipeline is made by 3D printing technology, which is cheap and convenient replacement. At the interface of the pipe, there is a sponge for filtering water vapor and our breathing pipe is replaceable for period.

In future, above mentioned limitations will be further studied. We will work on a further verification of proposed methods in the real systems, including interference factors, design for adults and children, the use of breathing pipe cycle. Additionally, considering a trend of intergrating this device into internet of things enabled healthcare system [32]–[35], we will focuse on the work of connecting this device into a hetegenous internet of things environment, and cooperate with the hospital for clinical testing and date analysis in the future.

VI. CONCLUSION

We describe a mainstream device for monitoring the respiratory flow in this paper. Respiratory flow monitoring with differential pressure methods can provide valuable information for diagnosis. New airway tube is designed when the acquisition of pressure singles is taken into consideration. BP neural network is used to fit the experimental results, and good linear relationship is obtained. It is proved that comparing with the least square method, BP neural network can be used in more complex function which is used for calculating the target value. A host of experiments and tests show that the designed mainstream device can accurately monitor respiration and acquire stable and real-time signals.

REFERENCES

[1] WHO.Int. (2016). *Chronic Respiratory Diseases*. Accessed: Jun. 13, 2016. [Online]. Available: http://www.who.int/respiratory/en/

[2] X. Wang and S. Wang, "Hierarchical deployment optimization for wireless sensor networks," *IEEE Trans. Mobile Comput.*, vol. 10, no. 7, pp. 1021–1041, Jul. 2011.

[3] M. B. Jaffe and J. Orr, "Continuous monitoring of respiratory flow and CO_2," *IEEE Eng. Med. Biol. Mag.*, vol. 29, no. 2, pp. 44–52, Mar./Apr. 2010.

[4] Z. Cao, R. Zhu, and R.-Y. Que, "A wireless portable system with microsensors for monitoring respiratory diseases," *IEEE Trans. Biomed. Eng.*, vol. 59, no. 11, pp. 3110–3116, Nov. 2012.

[5] J. Yang, H. Wang, B. Wang, and L. Wang, "Accurate and stable continuous monitoring module by mainstream capnography," *J. Clin. Monitor. Comput.*, vol. 28, no. 4, pp. 363–369, 2014.

[6] M. Pekdemir, O. Cinar, S. Yilmaz, E. Yaka, and M. Yuksel, "Disparity between mainstream and sidestream end-tidal carbon dioxide values and arterial carbon dioxide levels," *Respiratory Care*, vol. 58, no. 7, pp. 1152–1156, 2013.

[7] Y. S. Lee, P. N. Pathirana, C. L. Steinfort, and T. Caelli, "Monitoring and analysis of respiratory patterns using microwave Doppler radar," *IEEE J. Transl. Eng. Health Med.*, vol. 2. 2014, Art. no. 1800912.

[8] J. Hodgkinson, R. Smith, W. O. Ho, J. R. Saffell, and R. P. Tatam, "Non-dispersive infra-red (NDIR) measurement of carbon dioxide at 4.2 μm in a compact and optically efficient sensor," *Sens. Actuators B, Chem.*, vol. 186, pp. 580–588, Sep. 2013.

[9] J. Yang, H. Wang, B. Chen, B. Wang, and L. Wang, "Use of signal decomposition to compensate for respiratory disturbance in mainstream capnometer," *Appl. Opt.*, vol. 53, no. 10, pp. 2145–2151, 2014.

[10] J. Yang, B. Chen, K. Burk, H. Wang, and J. Zhou, "A mainstream monitoring system for respiratory CO_2 concentration and gasflow," *J. Clin. Monitor. Comput.*, vol. 30, no. 4, pp. 467–473, 2016.

[11] J. Yang, B. Chen, J. Zhou, and Z. Lv, "A low-power and portable biomedical device for respiratory monitoring with a stable power source," *Sensors*, vol. 15, no. 8, pp. 19618–19632, 2015.

[12] P. Grossman, "The LifeShirt: A multi-function ambulatory system monitoring health, disease, and medical intervention in the real world," *Studies Health Technol. Inform.*, vol. 108, pp. 133–141, Aug. 2004.

[13] C. F. Clarenbach, O. Senn, T. Brack, M. Kohler, and K. E. Bloch, "Monitoring of ventilation during exercise by a portable respiratory inductive plethysmograph," *Chest*, vol. 128, no. 3, pp. 1282–1290, 2005.

[14] L. Kent, B. O'Neill, G. Davison, A. Nevill, J. S. Elborn, and J. M. Bradley, "Validity and reliability of cardiorespiratory measurements recorded by the LifeShirt during exercise tests," *Respirat. Physiol. Neurobiol.*, vol. 167, pp. 162–167, Jun. 2009.

[15] J. Orr, S. Kofoed, and D. Westenskow, "A respiratory flowmeter based on a modified mainstream CO2 cuvette," *J. Clin. Monitor.*, vol. 9, no. 3, p. 215, 1993.

[16] U. Rannik *et al.*, "Intercomparison of fast response commercial gas analysers for nitrous oxide flux measurements under field conditions," *Biogeosci. Discussions*, vol. 11, no. 8, pp. 11747–11783, 2014.

[17] S. M. Hartmann, R. W. Farris, J. L. Di Gennaro, and J. S. Roberts, "Systematic review and meta-analysis of end-tidal carbon dioxide values associated with return of spontaneous circulation during cardiopulmonary resuscitation," *J. Intensive Care Med.*, vol. 30, no. 7, pp. 426–435, 2015.

[18] S. Cui, M. Cohen, P. Stabat, and D. Marchio, "CO_2 tracer gas concentration decay method for measuring air change rate," *Building Environ.*, vol. 84, pp. 162–169, Jan. 2015.

[19] S. Alshaban and R. Ali, "Using neural and fuzzy software for the classification of ECG signals," *Res. J. Appl. Sci. Eng. Technol.*, vol. 2, no. 1, pp. 5–10, 2010.

[20] A. Turnip, K.-S. Hong, and S. S. Ge, "Backpropagation neural networks training for single trial EEG classification," in *Proc. IEEE 29th Chin. Control Conf. (CCC)*, Jul. 2010, pp. 2462–2467.

[21] P. K. Padhy, A. Kumar, V. Chandra, K. R. Thumula, and A. Kumar, "Feature extraction and classification of brain signal," *World Acad. Sci. Eng. Technol.*, vol. 55, pp. 651–652, Jun. 2011.

[22] H. Zhang, M. Chang, J. Wang, and S. Ye, "Evaluation of peach quality indices using an electronic nose by MLR, QPST and BP network," *Sens. Actuators B, Chem.*, vol. 134, no. 1, pp. 332–338, 2008.

[23] H. L. Hu, J. Dong, J. Zhang, Y. J. Cheng, and T. M. Xu, "Identification of gas/solid two-phase flow regimes using electrostatic sensors and neural-network techniques," *Flow Meas. Instrum.*, vol. 22, no. 5, pp. 482–487, 2011.

[24] Y.-L. Hou *et al.*, "Improvement of BP neural network by LM optimizing algorithm in target identification," *J. Detection Control*, vol. 1, p. 12, Jan. 2008.

[25] X. Liu, X. Yan, Z. Yu, G. Qin, and Y. Mo, "Keyword extraction for Web news documents based on LM-BP neural network," in *Proc. 27th Chin. IEEE Control Decision Conf. (CCDC)*, May 2015, pp. 2525–2531.

[26] H. Zhang, D. Xu, and Y. Zhang, "Boundedness and convergence of split-complex back-propagation algorithm with momentum and penalty," *Neural Process. Lett.*, vol. 39, no. 3, pp. 297–307, 2014.

[27] E. Kuriscak, P. Marsalek, J. Stroffek, and P. G. Toth, "Biological context of Hebb learning in artificial neural networks, a review," *Neurocomputing*, vol. 152, pp. 27–35, Mar. 2015.

[28] Q. Xie, J. Li, X. Gao, and J. Jia, "Fourier domain local narrow-band signal extraction algorithm and its application to real-time infrared gas detection," *Sens. Actuators B, Chem.*, vol. 146, no. 1, pp. 35–39, 2010.

[29] V. S. Kothnur, S. Mukherjee, and X. M. Yu, "Two-dimensional linear elasticity by the boundary node method," *Int. J. Solids Struct.*, vol. 36, no. 8, pp. 1129–1147, 1999.

[30] Y. Cheng and J. H. Li, "A complex variable meshless method for fracture problems," *Sci. China Phys., Mech. Astron.*, vol. 49, no. 1, pp. 46–59, 2006.

[31] X. Y. Mukherjee and S. Mukherjee, "On boundary conditions in the element-free Galerkin method," *Comput. Mech.*, vol. 19, no. 4, pp. 264–270, 1997.

[32] P. Yang *et al.*, "Lifelogging data validation model for Internet of Things enabled personalized healthcare," *IEEE Trans. Syst., Man, Cybern., Syst.*, vol. 48, no. 1, pp. 50–64, Jan. 2018.

[33] J. Qi, P. Yang, M. Hanneghan, and S. Tang, "Multiple density maps information fusion for effectively assessing intensity pattern of lifelogging physical activity," *Neurocomputing*, vol. 220, pp. 199–209, Jan. 2017.

[34] J. Qi, P. Yang, M. Hanneghan, D. Fan, Z. Deng, and F. Dong, "Ellipse fitting model for improving the effectiveness of life-logging physical activity measures in an Internet of Things environment," *IET Netw.*, vol. 5, no. 5, pp. 107–113, 2016.

[35] J. Qi, P. Yang, D. Fan, and Z. Deng, "A survey of physical activity monitoring and assessment using Internet of Things technology," in *Proc. IEEE Int. Conf. Pervasive Intell. Comput.*, Oct. 2015, pp. 2357–2362.